JOURNAL OF SOLID STATE CHEMISTRY 109, 345–351 (1994)

$La_6BaYCu_8O_{20}$: A New Oxygen Deficient Perovskite

R. J. Cava, H. W. Zandbergen,[1] R. B. Van Dover, J. J. Krajewski, T. Siegrist, W. F. Peck, Jr., R. S. Roth,[2] and R. J. Felder

AT&T Bell Laboratories, Murray Hill, New Jersey 07974

Received June 21, 1993; accepted August 6, 1993

$La_6BaYCu_8O_{20}$ is a new three-dimensional oxygen deficient perovskite related to the well-known three-dimensional material $La_4BaCu_5O_{13}$. The inclusion of a small rare earth results in an extension of the layerlike areas within the three-dimensional network. The same structure is also found for $La_6BaDyCu_8O_{20}$. The structure can be doped with Sr for La, or Ca for the small lanthanide. No superconductivity is observed down to 0.3 K. $La_4BaCu_5O_{13}$ and the new compound form the first two members of a new three-dimensional homologous series $La_{4+2n}BaLn_nCu_{5+3n}O_{13+7n}$ through the addition of "123" type structural units. © 1994 Academic Press, Inc.

INTRODUCTION

One of the well-established empirical criteria for the occurrence of high T_c superconductivity in cuprates is that the crystal structures must be layered. Many layered cuprates are known. The three-dimensional metallic perovskites (1–7) $LaCuO_{3-\delta}$, $La_4BaCu_5O_{13\pm x}$, $La_{8-x}Sr_xCu_8O_{20}$ ($1.3 \leq x \leq 1.9$), and $La_{3.4}Sr_{0.6}Cu_4O_{10}$ (prepared at elevated pressure) are not superconducting above 4.2 K, establishing an important distinction in behavior between two-dimensional and three-dimensional metals. To further explore the possibilities of three-dimensional materials, we have investigated what structures might occur upon the inclusion of smaller rare earths. We have found the new phase $La_6BaLnCu_8O_{20}$, for Y and Dy, where the eightfold coordination of the smaller rare earth has added a new wrinkle to the still-three-dimensional structure by extending planelike structural regions. The materials can be doped significantly with Sr and Ca, for La and the small rare earths, respectively, for example, to $La_{6-x}Sr_xBaYCu_8O_{20}$, $x = 0.6$, and $La_6BaY_{1-x}Ca_xCu_8O_{20}$, $x = 0.4$. The compounds are metallic conductors, and are not superconducting down to 0.3 K, even though the average formal Cu valence, 2.12^+ to 2.22^+, is exactly in the range in which high T_c superconductivity occurs in layered materials. The structure of the new phase is derived from that of $La_4BaCu_5O_{13}$ by the addition of an $La_2LnCu_3O_7$ "123" type structural unit. A new type of homologous series can be derived based on that principle, with formulae $La_{4+2n}BaLn_nCu_{5+3n}O_{13+7n}$, which become essentially two-dimensional 123 for large n.

[1] National Centre for High Resolution Electron Microscopy, Delft Institute of Technology, Delft, The Netherlands.

[2] National Institute of Standards and Technology, Gaithersburg, MD 20899, retired.

SYNTHESIS

Starting materials were freshly dried Ln_2O_3, alkaline earth carbonates, and CuO. Initial investigations of the La_2O_3–Dy_2O_3–BaO–CuO system revealed the existence of a distinct perovskite phase at relatively low Dy contents on being heated at temperatures near 1000° in O_2. A formula $La_6BaDyCu_8O_{20}$ was determined by high resolution electron microscopy of a small crystallite of the new phase, and a perovskite supercell with periods $4\sqrt{2}a_0 \times 2\sqrt{2}a_0 \times 2a_0$ and a non-90° angle between the long axes (where a_0 = the simple perovskite subcell of 3.8 Å) was determined. Samples with Y and Dy as examples of small rare earths were then synthesized at the determined stoichiometry $La_6BaLnCu_8O_x$, and at seven neighboring compositions with small differences in the La, Ba, Ln, and Cu contents. Only the samples at the stoichiometry consistent with the high resolution electron microscopy results were single phase. Because of the many other compounds known to form in this chemical system, some of which are superconducting, extensive mechanical grinding of the powders (agate mortar and pestle) and long heating times were employed to insure sample homogeneity. Typical heating schedules were (in flowing O_2) 900°C, 16 hr; 1000°C, 32 hr; and 1025°C, 75 hr (with intermediate grindings). Heating at 1045°C resulted in decomposition of the phase. The final heating was in pellet form for 16 hr at 1025°C. The same procedure was followed to synthesize samples of the type $La_{6-x}Sr_xBaLnCu_8O_{20}$ and $La_6BaLn_{1-x}Ca_xCu_8O_{20}$. For both rare earths, single phase material was obtained up to $x = 0.6$ for Sr substitutions, up to $x = 0.4$ for Ca for Y substitution, and $x = 0.6$ for Ca for Dy substitution.

The oxygen content of several representative sam-

0022-4596/94 $6.00
Copyright © 1994 by Academic Press, Inc.
All rights of reproduction in any form reserved.

ples was determined by reduction to Ln_2O_3 + BaO(SrO, CaO) + Cu metal in a 15% H_2–85% N_2 mixture in a commercial TGA. Oxygen contents of 19.9(1) per formula unit were found, which agrees with the structural model. Treatment in oxygen at 20 atm pressure at 700°C did not result in additional oxygen uptake.

ELECTRON MICROSCOPY

Thin specimens for electron microscopy were obtained by crushing and mounting the crystal fragments on a Cu grid covered with a carbon coated holey film. Electron diffraction was performed with a Philips CM30T electron microscope operating at 300 kV and equipped with a side-entry 25°/55° tilt specimen holder. High resolution electron microscopy (HREM) was carried out with a Philips CM30ST electron microscope operating at 300 kV and equipped with a field emission gun as the electron source and a side-entry 25°/25° tilt specimen holder.

The HREM images were recorded at a series of defocus values, and particularly at a defocus of about −40 nm at which all cations in [110] images are imaged as dark dots. Image calculations were carried out using a MacTempas software program, in which the following parameters were used: spherical aberration 1.2 mm, defocus spread 5 nm, objective aperture 6.5 nm^{-1}, beam convergence 0.4 mrad, and mechanical vibration 0.05 nm. The thickness and defocus were varied.

Electron diffraction, carried out with a number of crystals, which were rotated to scan the reciprocal space, showed the unit cell to be a superstructure of the perovskite structure. The unit cell was found to be monoclinic with $a \simeq 10.9$, $b \simeq 7.70$ ($\simeq 2 \times 3.85$), $c \simeq 12.2$, and $\beta \simeq 117°$. To show correspondence with the simple perovskite

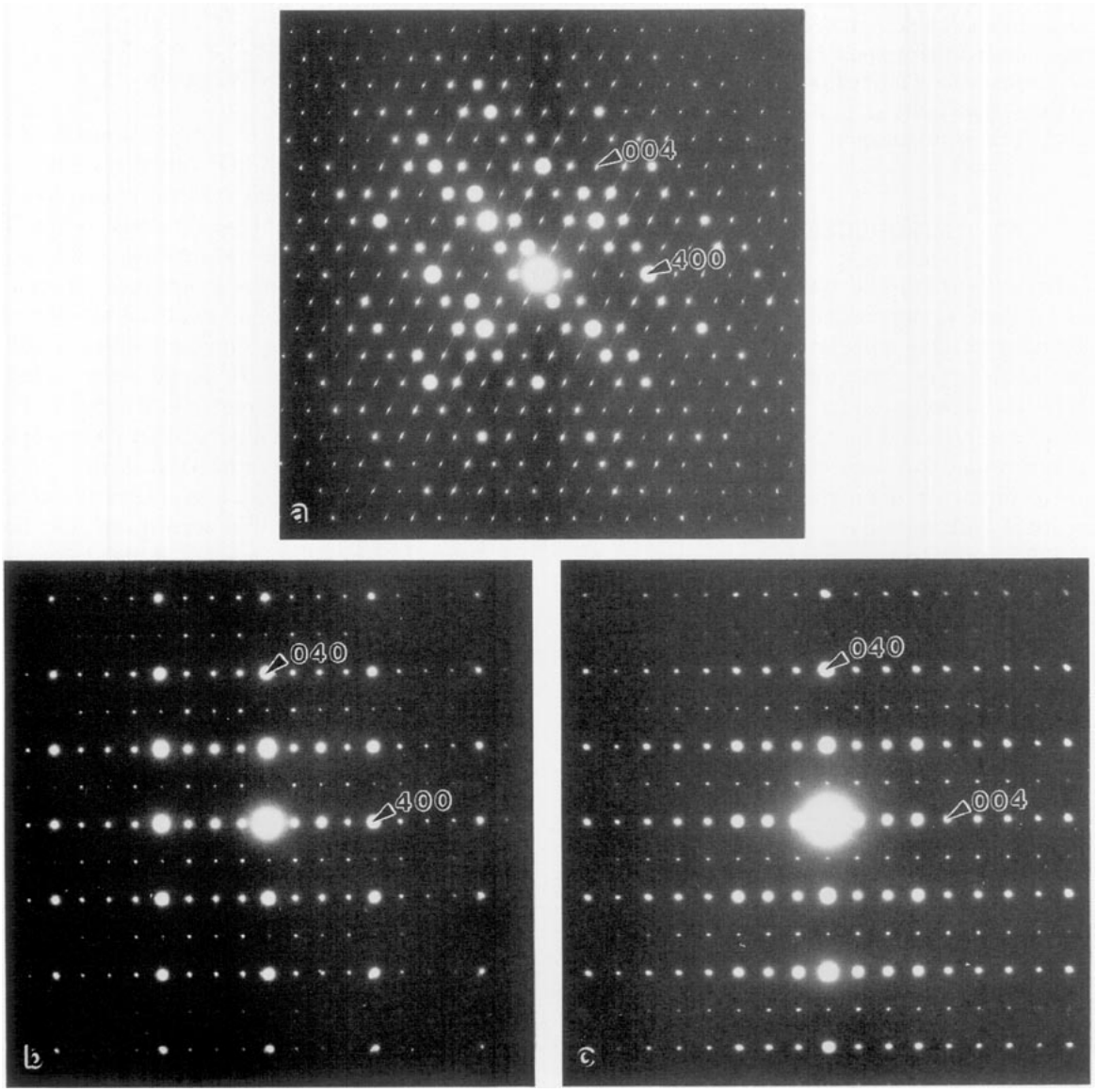

FIG. 1. Electron diffraction patterns of $La_6BaDyCu_8O_{20}$ along (a) [010], (b) [001], and (c) [100].

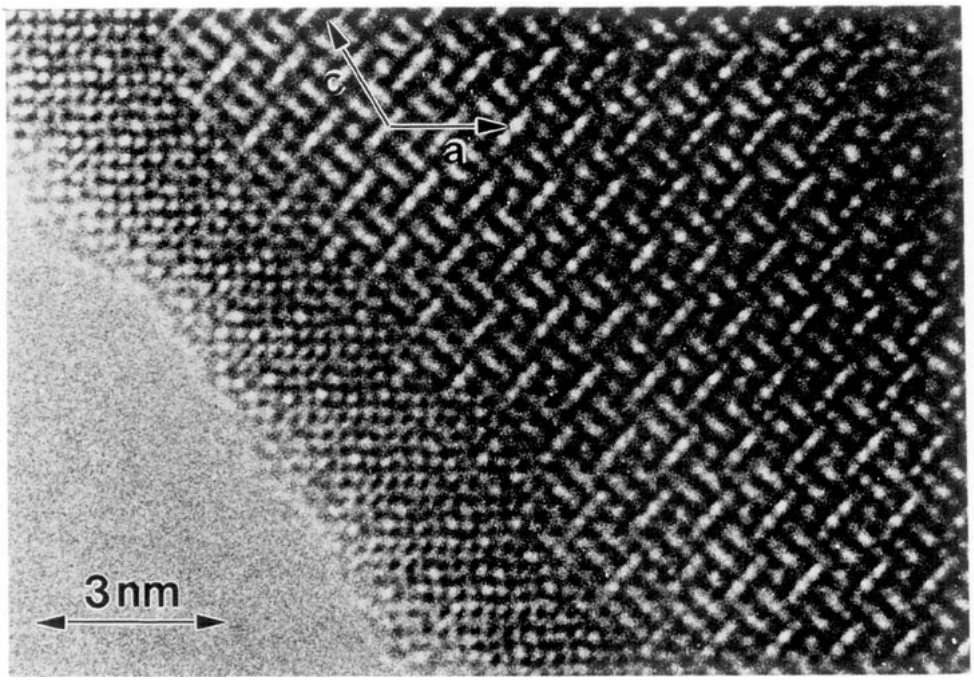

FIG. 2. [010] High resolution electron micrograph showing the structure image of $La_6BaDyCu_8O_{20}$. Conditions described in the text. The change in the image from left to right is due to a change in thickness.

subcell structure, a *B*-centered monoclinic cell of twice the volume, with $a = 2\,a_p\sqrt{2}$, $b = 2\,a_p$, $c = 4\,a_p\sqrt{2}$, and $\beta = 89°$, could also be chosen. Electron diffraction patterns of the [100], [010], and [001] orientations are shown in Fig. 1.

HREM done on crystals in [010] orientation showed, in the very thin regions, a perovskitelike structure. In the thicker regions, the superstructure is obvious. The structure image shown in Fig. 2 changes from left (very thin (2 nm)) to right (about 5 nm) due to the change in thickness. In the thicker part, one can observe three types of features: (i) isolated bright dots, (ii) pairs of bright dots connected by a relatively bright region, and (iii) a row of three bright dots connected again by relatively bright regions. An obvious possibility is that these relatively bright regions represent oxygen vacancies. In order to check this assumption, image calculations were carried out for the structures of $La_2Sr_6Cu_8O_{16}$ (8) and $La_4BaCu_5O_{13.16}$ (9), which also adopt superstructures due to oxygen vacancy ordering. The calculations showed that the assumption was correct and allowed the postulation of a structure model, which is shown in Fig. 3. Image calculations carried out with this model resulted in images that agreed well with the experimental ones. In these calculations, no discrimination was made between La, Ba, and Dy, since they have very similar scattering cross sections. Also, all atoms were kept at their positions in the ideal perovskite structure. Although the positions of the La, Ba, and Dy atoms could not be distinguished from the HREM images, a model could still be proposed, based on the sizes of La^{3+}, Ba^{2+}, and Dy^{3+} cations (1.2, 1.6, and 1.0 Å respectively) and on the oxygen coordinations of available sites. The three different sites, 6 tenfold, 1 twelvefold, and 1 eightfold oxygen-coordinated, suggest the occupancies of La, Ba, and Dy, respectively. This leads to the structure model of Fig. 3.

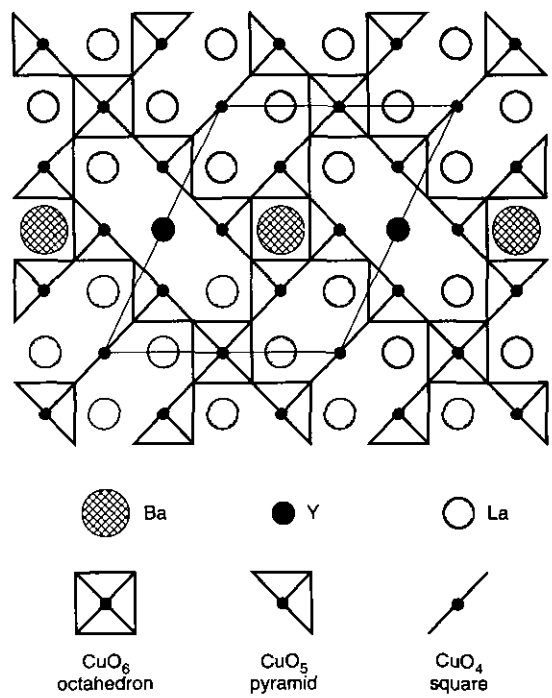

FIG. 3. The crystal structure (idealized) of $La_6BaDyCu_8O_{20}$. Copper coordination polyhedra as shown, unit cell outlined.

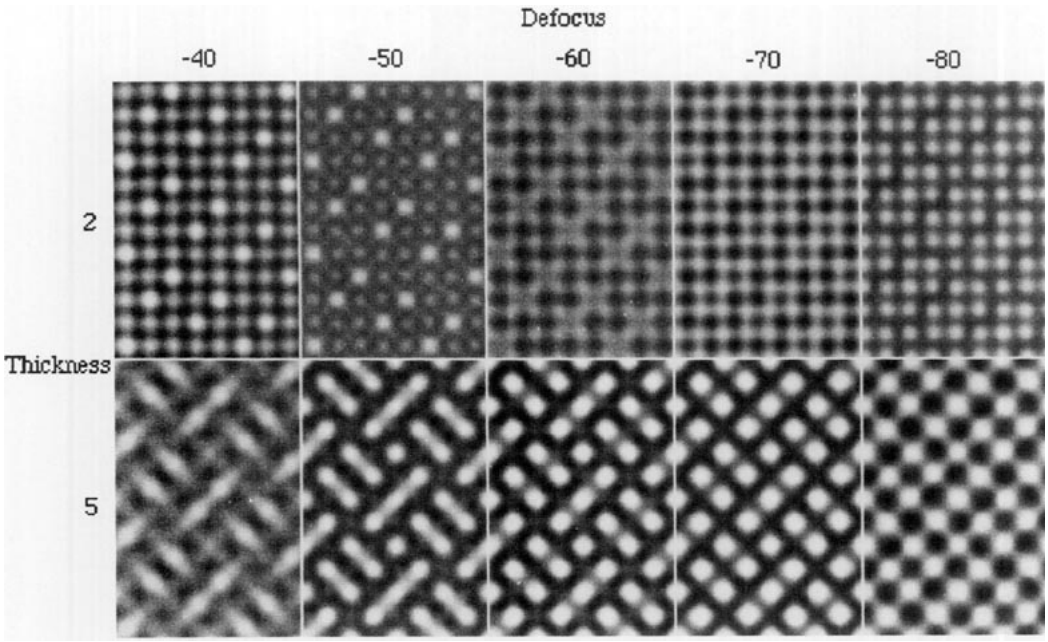

FIG. 4. Calculated images for the model structure shown in Fig. 3, for thicknesses of 2 and 5 nm and with various focus values. The calculated image with a thickness of 5 nm and a defocus of −40 nm agrees well with the experimental structure image in the middle of Fig. 2.

Apart from the superstructure in the a–c plane, a doubling of the b axis to twice the simple perovskite value is observed in electron diffraction patterns (see Figs. 1b and 1c). The reflections corresponding to this doubling are weak. The doubling is probably related to small tilts of the CuO_x polyhedra. Such tilts are quite common in perovskites to adjust the structure for the size of the large cation, which is too small for the "normal" 12-coordination.

POWDER X-RAY DIFFRACTION

A powder X-ray diffraction pattern for single phase $La_6BaDyCu_8O_{20}$ was taken on an automatic diffractometer with a focusing Guinier geometry with crystal monochromated Cu$K\alpha$ radiation. Due to the low symmetry and large volume of the true unit cell determined by electron microscopy, initial refinement of crystallographic cell parameters was for the simple perovskite subcell. Virtually all reflections present down to the 5% I_{max} level were indexed on the simple primitive orthorhombic subcell: a = 3.814(1), b = 3.869(1), and c = 3.858(1) Å, obtained by least-squares fitting to the data presented in Table 1.

Finding precise values of the supercell dimensions, even for the relatively high resolution diffraction pattern obtained, proved to be a problem due to the very close proximity of the b and c subcell dimensions (3.869 and 3.858 Å, respectively) and the pseudo-orthorhombic symmetry of the supercell. Selection of the shortest of the subcell axes (a = 3.814 Å) as the monoclinic unique (b) axis obviously did not account for the weak superlattice reflections. However, selection of either the subcell b axis or the subcell c axis as the monoclinic b axis of the supercell resulted in fits of equal quality to both the strong subcell and weaker supercell reflections for the now much larger true unit cell. Subcell reflections were assigned their new indices from the matrix relating subcell and supercells in real space, and refinement of the supercell dimensions was based on subcell derived reflections only, due to the large volume and low symmetry of the true cell. The indexing for one cell choice $(a, b, c)_{monocl.}$ = (2, 0, −2/0, 2, 0/1, 0, 3) $(a, b, c)_{subcell}$ is shown in Table 1. The true cell parameters refine to a = 10.851(7), b = 7.738(2), c = 12.187(6), β = 117.10(3)°. This cell chose twice the longest subcell (b) axis for the monoclinic b. Fits of equal quality with slightly different cell dimensions are obtained for a supercell choice with the monoclinic b axis equal to twice the subcell b axis, and different relationships between monoclinic supercell a and c and orthorhombic subcell a and c. For instance, choice of $(a, b, c)_{monocl.}$ = (−2, 0, −2/0, 2, 0/3, 0, −1) $(a, b, c)_{subcell}$ is also satisfactory. A very high resolution, high intensity powder diffraction experiment would have to be performed to distinguish the various nearly identical alternatives. Our attempts to grow single crystals by melting and various flux techniques were unsuccessful, but crystals would be expected to be seriously twinned.

HOMOLOGOUS SERIES

Figure 5 presents an idealization of the crystal structures of the compounds $La_4BaCu_5O_{13}$ and $La_6BaYCu_8O_{20}$

TABLE 1
Powder X-Ray Diffraction Pattern for $La_6BaDyCu_8O_{20}$ ($CuK\alpha_1$)

$2\theta_{obs}$[a]	I/I_0 (%)	Subcell index[b]	Subcell $2\theta_{calc}$	Supercell index[c]	Supercell $2\theta_{calc}$
9.04	0.5			$\bar{1}01$	
18.15	0.5			$\bar{2}02$	
22.13	0.5			102	
22.98	9	010	22.97	020	22.97
23.05	9	001	23.03	$\bar{2}03$	23.03
23.32	6	100	23.30	201	23.30
27.40	1			$\bar{3}03$, 121	
29.40	1			$\bar{2}22$	
29.60	2			220	
30.04	2			103	
32.75	67	011	32.75	$\bar{2}23$	32.75
32.90	71	110	32.95	221	32.95
32.98	100	101	33.00	004	33.00
33.92	4			023, $\bar{4}03$	
34.17	4			$\bar{3}22$, $\bar{4}01$+	
36.35	2			320?	
37.70	5			$\bar{2}24$	
37.97	7			222, $\bar{1}24$	
39.75	2			$\bar{3}24$	
40.55	20	111	40.59	024	40.59
41.30	4			$\bar{4}05$, $\bar{4}23$	
41.87	4			401, $\bar{5}02$	
43.75	1			$\bar{5}01$, $\bar{4}24$+	
44.90	3			$\bar{3}25$, $\bar{1}25$+	
45.37	4			303	
46.87	14	020	46.92	040	46.93
47.06	26	002	47.07	$\bar{4}06$	47.06
47.64	13	200	47.65	402	47.65
52.52	3			142, $\bar{5}25$	
52.90	3	021	52.90	$\bar{2}43$	52.90
53.05	6	120	53.03	241	53.03
53.05		012	53.00	$\bar{4}26$	53.00
53.17	6	102	53.17	$\bar{2}07$	53.16
53.53	4	210	53.53	422	53.53
53.60	4	201	53.56	205	53.56
58.50	19	121	58.56	044	58.56
58.62	39	112	58.65	$\bar{2}27$	58.65
59.07	18	211	59.02	225	59.02
68.65	9	022	68.65	$\bar{4}46$	68.65
69.03	3?	220	69.11	442	69.11
69.22	11	202	69.22	008	69.22
78.02	3	031	78.06	$\bar{2}63$	78.06
78.28	8	130	78.17	261	78.17
78.28		013	78.28	$\bar{6}29$	78.27
78.42	8	103	78.41	$\bar{4}010$	78.40
79.26	5	301	79.27	406	79.28
79.26		310	79.25	623	79.25

[a] Weak supercell reflections included to $2\theta = 55°$.

[b] Orthorhombic perovskite subcell, $a = 3.814(1)$, $b = 3.869(1)$, $c = 3.858(1)$.

[c] True monoclinic supercell, $a = 10.851(8)$, $b = 7.738(2)$, $c = 12.187(6)$, $\beta = 117.10(3)°$. Super- and subcells related by $(a, b, c)_{super} = (2, 0, -2/0, 2, 0/1, 0, 3)\ (a, b, c)_{sub}$. Reflections for doubling b are very weak, so no odd K reflections are seen in the powder X-ray pattern.

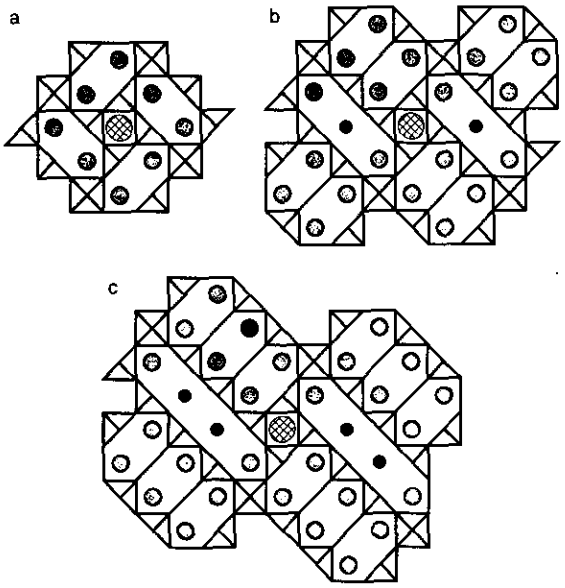

FIG. 5. The principle of the homologous series $La_{4+n}BaY_nCu_{5+n}O_{13+7n}$. Shown are the known structures for (a) $La_4BaCu_5O_{13}$, $n = 0$, and (b) $La_6BaYCu_8O_{20}$, $n = 1$, and the hypothetical compound (c) $La_8BaY_2Cu_{11}O_{27}$, $n = 2$.

and the hypothetical compound $La_8BaY_2Cu_{11}O_{27}$. The figure shows that the crystal structure of $La_6BaYCu_8O_{20}$ can be derived from that of $La_4BaCu_5O_{13}$ by addition of slabs of stoichiometry $La_2YCu_3O_7$ with the 123 O_7 crystal structure, a single *b* unit cell wide and infinite along *a* and *c*. This slab extends the microscopic layerlike aspect of the three-dimensional $La_4BaCu_5O_{13}$ crystal structure. Taking this building principle further through the addition of another $La_2YCu_3O_7$ slab results in a stoichiometry $La_8BaY_2Cu_{11}O_{27}$ with a crystal structure shown in Fig. 5c. The homologous series has the formula $La_{4+2n}BaLn_nCu_5O_{13+7n}$ where *Ln* is a small rare earth; $n = 0$ and $n = 1$ are the known compounds. For $n = 2$, the complexity of the crystal structure suggests that the actual occurrence or nonoccurrence of this phase may depend critically on synthesis temperature and chemistry (such as partial substitution of Sr for La). At some point, a mixture of low *n* material and a layered $n = \infty$ material of the 123 type structure will become more stable than the complex homologous series compound.

ELECTRICAL RESISTIVITY

Samples were first tested for superconductivity down to 4.2 K by ac susceptibility. No superconductivity was observed. Resistivities were measured on single phase polycrystalline pellets of $La_{6-x}Sr_xBaYCu_8O_{20}$, $La_6BaY_{1-x}Ca_xCu_8O_{20}$ and their Dy analogs in four-terminal dc measurements. The results are summarized in Figs. 6–8. For the undoped materials, the resistivities are relatively high but are metallic in character until 100 K for

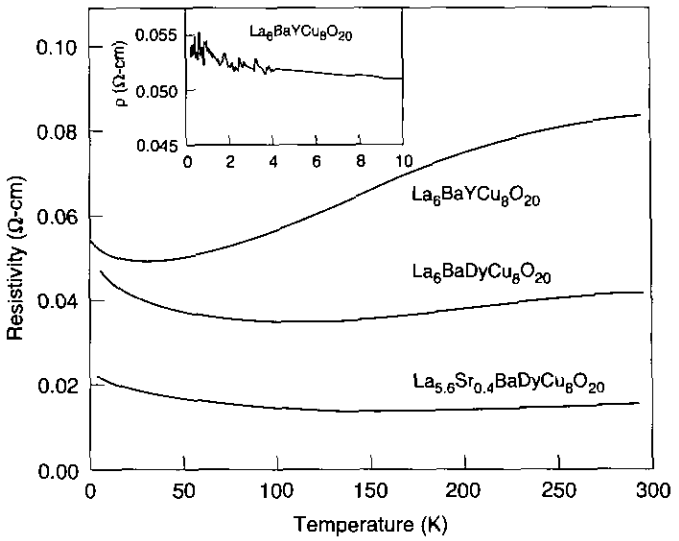

FIG. 6. The temperature dependent resistivities of $La_6BaYCu_8O_{20}$, $La_6BaDyCu_8O_{20}$, and $La_{5.6}Sr_{0.4}BaDyCu_8O_{20}$ polycrystalline pellets.

Dy or 20 K for Y, when semiconducting behavior is then observed. Introduction of further carriers through Sr or Ca doping results in a dramatic decrease in the resistivity. At the highest doping levels, as shown in Fig. 8, the resistivities are very low but the temperature dependencies are not really metallic. The low temperature upturns may be due to either grain boundary or intrinsic localization effects. Even the best resistivities are significantly higher than that which is observed for polycrystalline $La_4BaCu_5O_{13}$, which has a higher formal copper oxidation state.

Figures 6–8 show, in insets, the resistivities for several representative samples between 4.2 and 0.3 K. The mini-

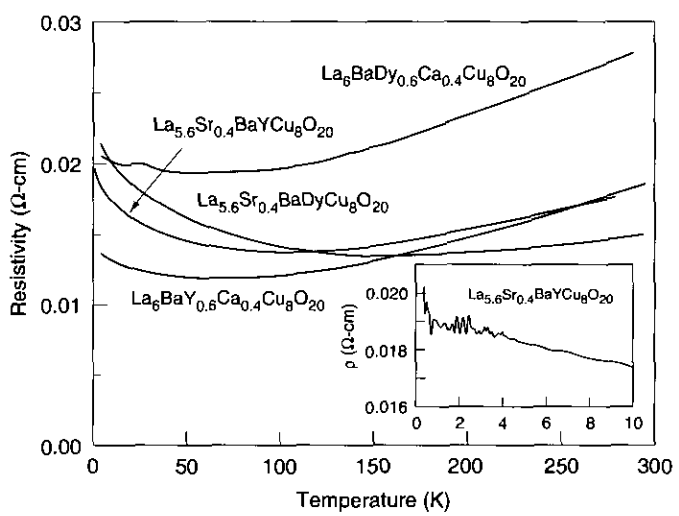

FIG. 7. The temperature dependent resistivities for moderately doped oxygen deficient perovskites $La_{6-x}Sr_xBaLnCu_8O_{20}$ and $La_6BaLn_{1-x}Ca_xCu_8O_{20}$.

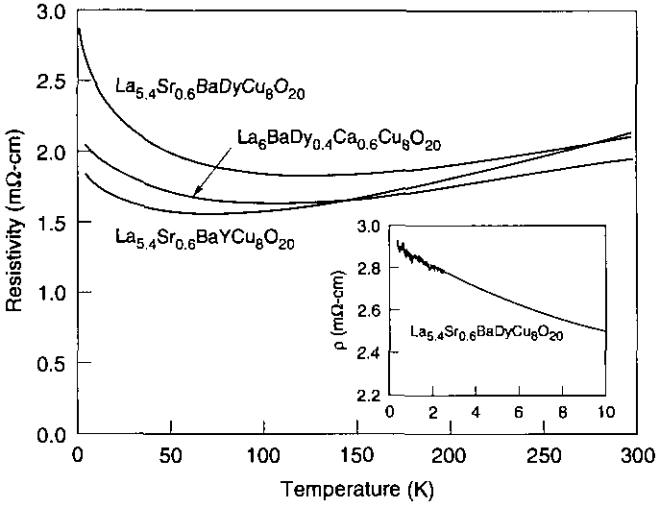

FIG. 8. The temperature dependent resistivities for the most heavily hole-doped perovskites $La_{6-x}Sr_xBaLnCu_8O_{20}$ and $La_6BaLn_{1-x}Ca_xCu_8O_{20}$.

mum temperature, 0.3 K, is two orders of magnitude lower than the temperature at which typical layered copper oxides become superconducting. The data are noisy due to the very high contact resistance below 4 K and the need to use a low current to avoid heating. Nevertheless, it is clear that the samples do not become superconducting. Thus the present materials, which are three-dimensional but contain substructural regions which are two-dimensional in character, are further confirmation of the importance of fully two-dimensional crystal structures for the occurrence of high T_c superconductivity.

CONCLUSIONS

We have reported the existence of a new three-dimensional copper oxide related to $La_4BaCu_5O_{13}$ with a somewhat larger two-dimensional structural component due to the inclusion of a smaller rare earth. The compounds can be made metallic by suitable doping but do not become superconducting down to 0.3 K. The existence of another member of a homologous series can be predicted. Our attempts to synthesize it have not yet succeeded. We expect that further experimentation with oxygen deficient perovskites which mix rare and alkaline earth ions with different oxygen coordination requirements will result in the discoveries of a variety of compounds related to the ones described here.

REFERENCES

1. G. Demazeau, C. Parent, M. Pouchard, and P. Hagenmuller, *Mater. Res. Bull.* **7,** 913 (1972).
2. C. Michel, L. Er-Rakho, and B. Raveau, *Mater. Res. Bull.* **20,** 667 (1985).
3. L. Er-Rakho, C. Michel, and B. Raveau, *J. Solid State Chem.* **73,** 514 (1988).
4. J. F. Bringley, B. A. Scott, S. J. LaPlaca, R. F. Boehme, T. M. Shaw, M. W. McElfresh, and D. E. Cox, *Nature* **347,** 263 (1990).
5. P. K. Davies and C. M. Katzan, *J. Solid State Chem.* **88,** 368 (1990).
6. K. Otzschi and Y. Ueda, *J. Solid State Chem.* **107,** 149 (1993).
7. J. F. Bringley, B. A. Scott, S. J. LaPlaca, T. R. McGuire, F. Mehran, M. McElfresh, and D. E. Cox, *Phys. Rev. B47* **15,** 269 (1993).
8. W. T. Fu, D. J. W. Ijdo, and R. J. Helmholdt, *Mater. Res. Bull.* **27,** 287 (1992).
9. C. Michel, L. Er-Rakho, M. Hervieu, J. Pannetier, and B. Raveau, *J. Solid State Chem.* **68,** 143 (1987).